

DSM AND ORTHOIMAGES FROM QUICKBIRD AND IKONOS DATA USING RATIONAL POLYNOMIAL FUNCTIONS

Manfred Lehner, Rupert Müller, Peter Reinartz
German Aerospace Center (DLR), Remote Sensing Technology Institute, D-82234 Wessling, Germany
Manfred.Lehner@dlr.de

Commission I, WG I/5

KEY WORDS: rational polynomial functions, orthoimages, digital surface models, QUICKBIRD, IKONOS

ABSTRACT:

The rigorous approach for the derivation of digital surface models (DSM) and orthoimages from satellite and airborne scanner imagery via full modelling of the imaging process requires the knowledge of exterior and interior orientation of the camera. For IKONOS and QuickBird this basic data is not (fully) available to the user. Instead, rational polynomial functions (RPF) in standard form are provided as a substitute for describing the relationship between image and object space. To be able to derive DSM and orthoimages for this type of data even in the absence of appropriate ground control, software based on RPF has been developed. The software allows a lot of datums and projections for input and output data. This is important for worldwide application e.g. in case of catastrophes. The paper shows that a RPF is very near to linear in the object space variables longitude, latitude and height. This explains a large convergence radius and a rapid convergence in case of forward intersection. Residuals in image space from forward intersection are small and nearly constant in case of the GEO IKONOS-2 images tested. Large (also nearly constant) residuals in case of the QuickBird stereo pair can be used for a relative correction of the RPF either using residuals from verticality constraints with manually measured top/foot tie point pairs of large buildings or from forward intersection of a set of excellent tie points from matching. These corrected RPF can then be used to create a self-consistent set of DSM and orthoimages. The DSM derived from the high resolution data via RPF processing have been compared to best DSM available which was in most cases a C-Band SRTM model. Estimated mapping accuracy was found to correspond with the promises of the image provider in the case of available ground control.

1. INTRODUCTION

1.1 Motivation for RPF usage

The main motivation to deal more extensively with rational polynomial functions (RPF) lies in their tight connection to high resolution satellite imagery (HRSI) of the new commercial satellites IKONOS-2 and QuickBird. RPF have been discussed much earlier in searching for universal sensor models (USM) which should allow the user to deal with various sources of imagery in a unified approach without having to know about details of interior and exterior orientation of the sensor systems by which the images have been taken. Just a simple substitute for the collinearity equations and directly connecting 3D object space and 2D image space without having to bother about the series of coordinate transformations included in the rigorous approach (compare Müller, 2002). As RPF are adopted now as USM for HRSI and, furthermore, providers of HRSI are not disclosing full information on interior and exterior orientation of their sensors people are forced to use RPF. Meanwhile, it has been shown that for those small areas covered by HRSI scenes the accuracies of products like orthoimages and digital surface models (DSM) derived with RPF can meet the accuracies of the rigorous approach if some improvements are made by ground control information (Eisenbeiss, 2004). The main reason lies in the availability of high precision orbit and attitude determination using GPS in combination with gyros and startrackers of high performance.

The latter improvements made it possible to directly georeference HRSI with an accuracy which is sufficient for a series of applications, e.g. as basic map material in case of natural catastrophes. Here often a lack of time and accessibility are hindering the collection of ground control. Thus, it is also

an interesting question what can be improved on RPF even in the absence of ground control.

2. RPF BASIC EQUATIONS AND PROPERTIES

The RPF provided with the high resolution satellite images connect image space and object space by:

$$(1) \quad \text{row or column} = rpf(\lambda, \varphi, h)$$

where row/column are the image coordinates and λ , φ , and h are longitude, latitude and ellipsoidal height in geographic coordinates of WGS84 datum. For numerical reasons calculation is actually based on normalized variables restricted to $[-1,+1]$ interval by choosing appropriate values for offset and scale. Each of the RPF for row and column in equation (1) is given via a ratio of 2 polynomials of third order in normalized λ , φ , and h with 20 coefficients. RPF are provided in standard format (same sequence) for IKONOS-2 and Quickbird images. Details are given in (Grodecki et al., 2004).

To be able to investigate the potential of RPF, software has been developed with the following scope:

- Derivation of orthoimages (RPF and digital surface model (DSM) given) in any datum/projection
- "forward intersection" of multiple stereo tie points (RPF for each image given, DSM may be provided for initial values of heights and comparison of output heights)
- RPF correction based on ground control points (datum/projection can be variable; constant shifts are estimated in row and column direction)

- Special program for iterative least squares adjustment to retrieve heights of buildings and corrections to RPF from measurements of top/foot tie point pairs (verticality constraint)

For forward intersection and verticality constraint the basic linear observation equations of the iterative least squares adjustment are of the type:

$$(2) \quad \frac{\partial rpf}{\partial \lambda} \Delta \lambda + \frac{\partial rpf}{\partial \varphi} \Delta \varphi + \frac{\partial rpf}{\partial h} \Delta h = -rpf(\lambda, \varphi, h) + \text{row or column} + \text{residual}$$

where row/column are the measured image coordinates of tie points – normally found by automated image matching. Initial approximations for the object space coordinates (longitude λ , latitude φ , height h) are taken from an affine transformation based on the corner coordinates supplied with the imagery (longitude, latitude) and from given DSM (height) if available. If no DSM is available a constant mean height value can be taken without hindering convergence to the same values. The advantage of a DSM is the possibility of a direct check of all generated object space heights against the input DSM. The convergence is very rapid (in most cases 2 iterations are sufficient) because the first derivatives of the RPF are quite dominant. E.g. the vector of the first derivatives with respect to height is - over the whole image - nearly identical to the projection of a unit height vector onto the image plane in direction of the line of sight. Figure 1 shows an example for a derivative with respect to height for an IKONOS-2 image of Ortler mountain range (factor 50 enlarged). Figure 2 shows the variations left when the mean of the first derivative is subtracted from the vectors in figure 1 (same unit, factor 2000 enlarged!).

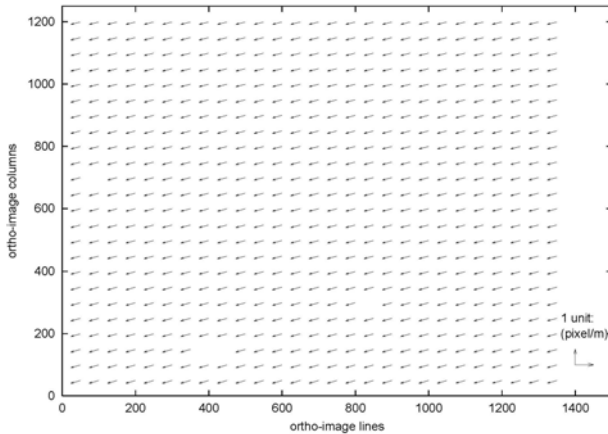


Figure 1: Vector plot of derivatives of RPF with respect to height for Ortler mountain range

Some numbers for the Ortler case (left image of IKONOS-2 stereo pair; pixel spacing 1 m; σ : standard deviation):
 Mean of h-derivative of row-RPF: $a = -0.506$ (stddev. 0.0016)
 Mean of h-derivative of col-RPF: $b = -0.161$ (stddev. 0.0056)
 Nominal collection elevation: $\gamma = 62.00507$
 Nominal collection azimuth: $\alpha = 163.5821$

$$\sqrt{a^2 + b^2} - \text{tg}(90 - \gamma) = 0.0006$$

$$\text{arctg}(b/a) = 180 - 17.65 = 162.35$$

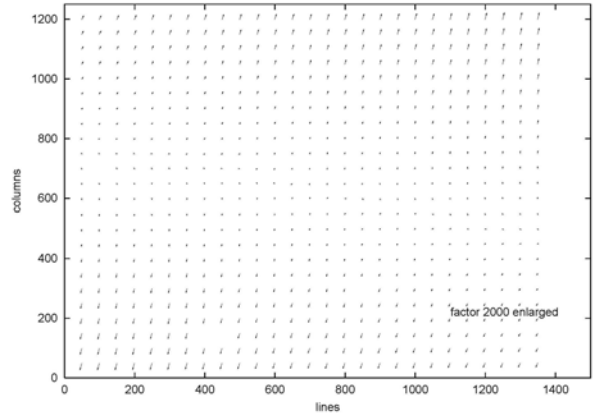


Figure 2: Mean vector is subtracted from the vectors in figure 1.

The derivatives with respect to latitude and longitude are similarly nearly constant over the small patches of HRSI. The values of these derivatives describe in good first approximation simply the translation from latitude/longitude grid into the pixel dimensions.

Thus, even when at first look the RPF are looking rather complex they are in reality very near to linear functions. This explains that they can be substituted with good success by affine transformations as investigated in Eisenbeiss, 2004 and Yamakawa, 2004.

In the stereo case this linearity leads to nearly constant residuals when applying iterative least squares adjustment using observation equations of type (2). In the Ortler case (height variation over the scene about 1650m) the residuals in image space of about 65000 tie points of high quality (sub-selected from a larger set) found by automated matching are given in table 1 for one stereo partner (point symmetric for the other). The residuals and their standard deviations are very small. The residuals beyond 0.5 pixel are due to blunders. If the 10 points with the largest residuals are removed (tested to be blunders or to lie in steep terrain) the min/max residuals drop below 0.5 pixel (second part of table 1). This type of removal of blunders is similar to the same practice in forward intersection using the rigorous approach.

Table 1: 65000 residuals (in pixel) of RPF forward intersection in IKONOS-2 Ortler stereo case

row residuals				column residuals			
mean	σ	min	max	mean	σ	min	max
0.03	0.03	-0.09	0.72	0.10	0.10	-0.34	2.71
10 points with maximum residuals in image space removed:							
0.03	0.03	-0.09	0.13	0.10	0.10	-0.34	0.47

The mean of the differences of SRTM C-Band DSM and the heights from forward intersection for these 65000 points is 7.6m with a standard deviation of 5.7m. The latter is in the order of the accuracy of the C-Band DSM

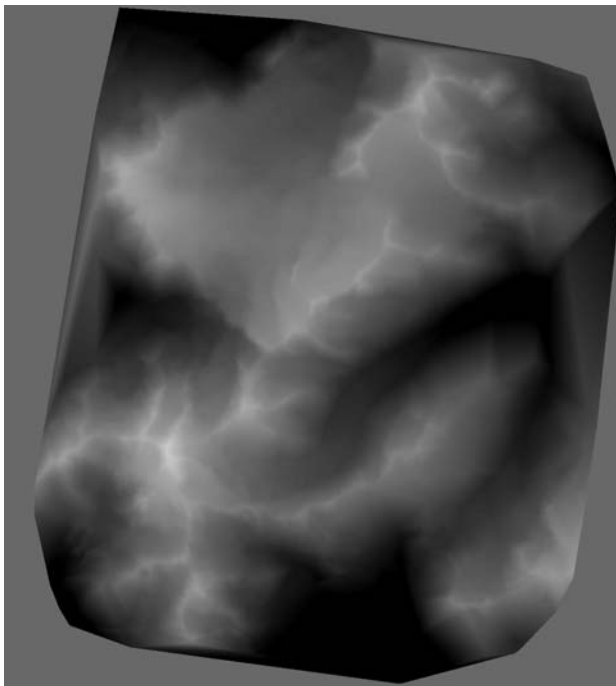
By region growing about 4500000 tie points have been derived and converted into object space coordinates by forward intersection with RPF. The DSM is shown in figure 3. Table 2 gives the residuals from forward intersection for all mass tie points. Certainly, the large min/max values are due to wrong matches in the mass tie point set. In the case of HRSI stereo partners mass tie points based on region growing will contain blunders, a value of 1% is certainly realistic. In table 2 less than

0.5% with largest residuals in image space during forward intersection have been removed leading to a drastic dropping of the minimum/maximum values of the residuals given in the lower part of table 2. One can base a blunder reduction procedure on this.

Table 2: Same as table 1 but for 4500000 tie points

row residuals				column residuals			
mean	σ	min	max	mean	σ	min	max
-0.03	0.08	-8	7	-0.09	0.28	-28	27
22000 points with largest residuals removed:							
-0.03	0.04	-0.3	0.3	-0.09	0.14	-1	1

Figure 3: DSM derived from mass tie points in Ortler case



Verticality constraints (heights of buildings)

If there are high buildings in the stereo images one can use a special “verticality constraint” on top/foot stereo tie point pairs. Object space lateral coordinates have to be identical for such a top/foot pair. An iterative least squares adjustment with 8 observation equation of type (2) for one top/foot pair (for 2 stereo partners, 4n observation equations for n stereo partners) and the four unknowns (latitude, longitude and the two heights) can be taken to compute the height of the buildings and to define relative corrections to a set of RPF.

3. CASE STUDIES

3.1 Munich: Improvement by Ground Control

The only data material where ground control data have been available was a set of three IKONOS-2 images of the city area of Munich (see table 3). 8 ground control points and several edges of buildings were measured in digitized aerial stereo photos on an analytical plotter of the TU Munich. Image coordinates have been measured always between all 3 pairs of the IKONOS-2 images on the screen using a measurement tool built into XDibias image processing system at DLR.

Table 3: Munich GEO IKONOS-2 image parameters

image	acquisition date	nom.col.azim.	nom.col.elev.
ik0	3/22/2003	126.9	61.4
ik1	6/10/2003	46.0	81.9
ik2	9/17/2003	1.1	65.6

The ground control points used lie within a circle of less than 1 km. Thus, only constant corrective shifts are estimated as recommended in (Eisenbeiss et al., 2004). The deviations of measured object space coordinates of these GCP from calculated ones on the basis of manual stereo measurements in ik0/ik1/ik2 (Gauss-Krüger coordinates) are given in table 4.

Table 4: Difference in m of object space coordinates computed via RPF versus measured for different stereo pairings and before and after RPF correction

RPF used	Diff easting		Diff northing		Diff height	
	mean	σ	mean	σ	mean	σ
Ik0/1	5.7	0.8	-7.0	0.6	5.2	1.8
Ik0/1/2	6.4	0.6	-7.0	0.5	6.4	1.3
Ik0/1/2 RPFcor	0.0	0.6	0.0	0.5	-0.1	1.3

The corrections to the RPF found as means of the residuals when comparing RPF results based on measured object space coordinates with measurements in the imagery are listed in table 5 together with their standard deviations.

Table 5: RPF corrections estimated for the 3 Munich Ikonos images based on 8 GCP

image	row correction	col correction	stddev. rows	stddev columns
ik0	5.16	3.65	0.56	0.60
ik1	7.29	5.50	0.76	0.70
ik2	9.41	7.34	0.88	1.04

The effect of such a shift in row and column direction is a 3D-shift of the point cloud in the map coordinate system because the system is near to linear. Using corrected RPF the ground control points are reproduced with zero mean deviation in easting, northing and height and standard deviation as before (last row in table 4).

It was not possible to derive a dense set of stereo tie points between the 3 Munich images because of the bad quality of ik0 (thin clouds), the different seasons and the big perspective differences of the city scenery. A small chip of a laser DSM (figure 4) provided by TU Munich could be used to fully test orthoimage generation of the respective city area including buildings. Figures 5 and 6 show the original image chip and the orthoimage produced with corrected RPF. The ortho-corrections to the buildings can be clearly seen.

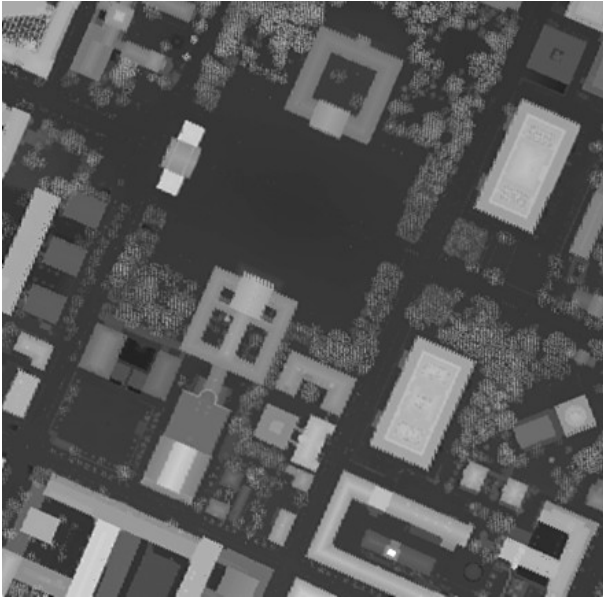


Figure 4: Laser DEM of Munich subarea (440m by 435 m)



Figure 5: chip from original image of approximately same area

Verticality constraints were used to calculate the heights of 15 buildings which could be compared to those measured on the analytical plotter. Experience was that it is difficult to measure top/foot tie point pairs because the foot often falls into shadow regions or may be obscured by other objects. The results given in the table below show that on average lower heights result from the measurement:

Mean height of the 15 buildings	RPF-heights - measured heights	
	mean	σ
18.9 m	-0.7 m	1.8 m



Figure 6: Orthoimage chip

Table 6 shows the statistic on the residuals from forward intersection of 124 reliable 3-fold tie points (found by matching). Once more the means of the residuals and their standard deviations are small.

Table 6: Residuals (pixel) from forward intersection of 124 3-fold tie points (common adjustment using 3 RPF) for the 3 Munich IKONOS images

row residuals				column residuals			
mean	σ	min	max	mean	σ	min	max
0.82	0.20	0.2	1.3	-0.54	0.15	-0.8	-0.2
-0.08	0.28	-0.6	0.7	-0.08	0.41	-1.3	0.7
-0.74	0.28	-1.4	-0.2	0.62	0.36	-0.1	1.5

3.2 Esfahan: relative improvement of RPF using tie points

A basic stereo pair of QuickBird images was available in this case (image parameters are given in table 7) and a DSM of SRTM C-Band (DSM0) from DLR database. Orthoimages produced with original RPF (RPF0) from the two images (time separation approximately 1 month) are not registered. By image correlation the mean shifts in first row of table 10 have been computed.

Table 7: QuickBird image parameters (pan, mean collected GSD 0.762 m and 0.731 m)

image	acquisition date	off-nadir angle	in-track	cross-track
QB04pan1	6/15/2004	29.0	29.0	1.4
QB04pan2	7/21/2004	-26.7	-26.5	-3.9

As no ground control points were available to do a RPF correction another way of at least relative correction has to be sought of. Verticality condition could be tried by measuring 5 big chimneys giving 5 top/foot stereo tie point pairs. The means and standard deviations of the individual residuals for each image are given in table 8. The derived heights of the chimneys lie between 38.7m and 80.1m.

Table 8: Mean and standard deviations (pixel) of residuals in image space from verticality constraints on 5 chimneys in QuickBird scenes (1pixel = 0.6 m)

row residuals				column residuals			
mean	σ	min	max	mean	σ	min	max
5.9	1.4	3.3	8.6	20.7	0.4	20.3	21.4
-5.6	1.4	-8.3	-3.0	-20.3	0.7	-21.5	-19.4

The means are now applied as corrections (constant shifts) to the RPF. There are difficulties in exactly measuring the coordinates of top/foot pairs of the chimneys in the stereo imagery. That can explain the larger standard deviation in row direction.

Corrected RPF (RPF1) are used to calculate a DSM1 with mass tie points from DLR matching software. On the basis of DSM and the corrected RPF orthoimages have been computed from the two imaging directions. These are then compared with each other by matching giving the small shifts in table 10. This shows that the relative correction of the RPF via the verticality constraint has generated a consistent situation.

Like in chapter 1.2 for Ortlter region we can also look at the residuals in image space when doing forward intersection with high quality tie points. The result is shown in table 9 for 13000 stereo tie points.

Table 9: Residuals (pixel) of RPF forward intersection in QuickBird stereo case (original RPF)

row residuals				column residuals			
mean	σ	min	max	mean	σ	min	max
4.07	0.04	3.2	6.2	20.9	0.20	16.7	31.7
-4.36	0.04	-6.6	-3.5	-20.6	0.20	-31.2	-16.5

This is very near to table 8 with much lower standard deviations. Thus, tie point corrected RPF (RPF2) are generated and DSM2 and orthoimages derived with this RPF2 version. The fit of the orthoimages is of equal quality as with RPF1 with slightly better mean shifts as can be seen in table 10. The DSM which would have been created directly by use of original RPF is identical to DSM2 because the nearly constant bias values are taken from forward intersection, that is the new RPF2 do intersect now with zero mean residuals in exactly the same points as resulted from forward intersection with original RPF. Thus, the relative correction is important only for orthoimage generation where correct intersection on the DSM surface is essential.

Table 10: Shifts between orthoimages generated with 3 different combinations of DSM and RPF

DSM	RPF version	Shifts between orthoimages (pixel = 0.6 m)				
		points	row	σ	column	σ
0	RPF0	47177	6.1	1.02	-14.3	0.97
1	RPF1	12871	-0.1	0.32	0.31	0.32
2	RPF2	13003	-0.2	0.34	0.0	0.34

Table 11 shows the mean and standard deviation of the differences of the object coordinate heights to DSM0-heights (DSM0-height – height from forward intersection) at the same lateral object space coordinates of the tie points (same tie points as in table 9).

Table 11: SRTM C-Band-heights minus heights from forward intersection for 13000 high quality tie points

RPF version	mean	σ
RPF0/RPF2	-16.8	2.9
RPF1	-19.0	2.9

With the stereo angles given in table 3 it is not possible to derive a valid DSM in built-up areas and in mountain areas with steep slopes. Thus, the excellent orthoimage fit given in table 10 is not indicating that buildings or steep mountain parts are rectified correctly. There is only a negligible success of matching of the orthoimages in these areas. To derive a valid DSM everywhere needs additional information e.g. more HRSI with different looking directions.

3.3 Cape Town: some DSM investigations

A GEO IKONOS-2 stereo pair was available for this region (1 m ground sampling distance). A digital surface model was interpolated from RPF based object space coordinates of mass tie points. The latter were generated with seed points from DLR matching software put into region growing process (Heipke, 1996). The region growing software was modified for high resolution imagery. In order to reduce blunders on edges and in homogenous areas Förstner interest operator was used with thresholds on roundness and variance of image chips to suppress intrusion into homogeneous areas. Low thresholds are to be taken in order to still allow most of the region growing to proceed normally (in case of Cape Town thresholds 0.3 for roundness of error ellipse and 15 for variance have been used – same procedure was used in the other HRSI stereo cases of this paper).

Orthoimages generated from the two looking directions using this RPF based DSM showed very small shifts (22340 points matched: row mean shift and σ : -0.26/0.48; column mean shift and σ : 0.30/0.24 pixel = m). The DSM is of poor quality in built-up areas with large buildings. This is not a RPF problem but a matching problem because of the large stereo angle between one-orbit stereo images of IKONOS. Figure 7 shows the DSM for a small area (about 800 m by 800 m) in the central city of Cape Town interpolated from about 44000 RPF-based object space coordinates of tie points from matching. For this sub-area including some tall skyscrapers manually measured points were added to the tie points from automated matching. A new DSM chip (figure 8) was interpolated from the results of forward intersection. In spite of being far from a decent DSM of this city area, the corresponding orthoimage chip shows some ortho-rectified skyscrapers. Whole streets are missing in the DSM and can not be reconstructed from this twofold stereo imagery because not one point can be matched even manually. No common parts can be seen in between the skyscraper images. Table 12 shows the statistic on the differences of DSM heights from SRTM and tie point heights from RPF. Of course, in the town area the standard deviation increases because of additional points on roofs not included in SRTM model of large grid size (about 90m).

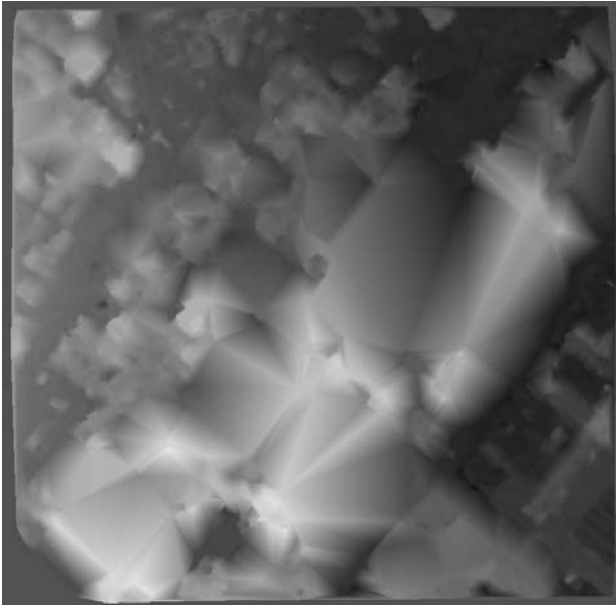


Figure 7: DSM from matching

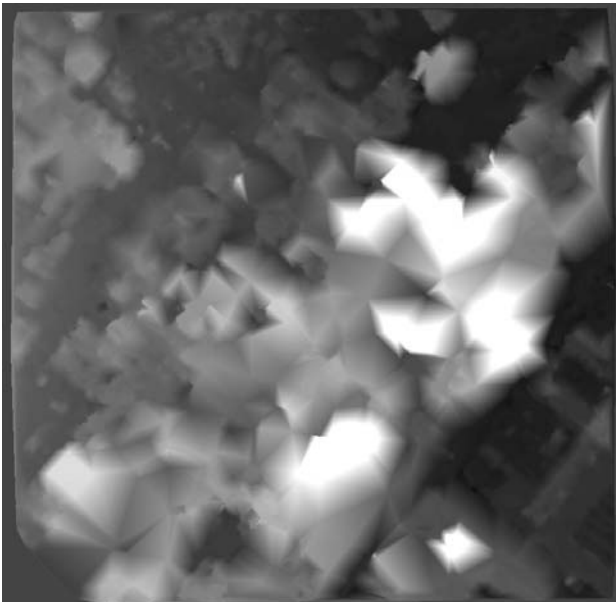


Figure 8: DSM from matching and 230 additional manual measurements

Table 12: DSM heights from SRTM minus DSM heights from RPF (Cape Town)

point type	points	min	max	mean	σ
Mass points	5470067	-134.0	137.1	-6.81	5.48
Best points	98960	-84.5	77.3	-6.17	5.34
Town area (matching)	44491	-40.8	22.0	-5.27	8.17
Town area (+manual)	44721	-120.3	22.0	-5.41	8.69

Verticality constraints have been applied for 30 manually measured top/foot tie point pairs leading to negligible shifts for the RPF (0.03 rows and 0.15 columns) very similar to those given for 13200 carefully sub-selected tie points as residuals

from forward intersection in table 13. Thus, the RPF intersect within the accuracy of the matching of the tie points. The heights of the buildings have been found to lie between 14.4 m and 122.9 m with a mean of 39.9 m. These are realistic values but cannot be checked because of missing ground truth.

Table 13: residuals from forward intersection

row residuals				column residuals			
mean	σ	min	max	mean	σ	min	max
0.01	0.03	-0.7	0.9	0.12	0.28	-6.4	8.1
80 points with largest residuals removed (blunders)							
0.01	0.01	-0.1	0.1	0.12	0.10	-0.9	0.9

4. CONCLUSIONS

The RPF are in all cases found to be very close to linear functions. The residuals in image space of mass tie points in forward intersection show small standard deviations. In case of the available IKONOS-2 images the mean residuals are also small (less 1 pixel). Reporting this to Space Imaging they confirmed that images delivered in the same package are subject to an at least relative block adjustment. In the multi-temporal QuickBird stereo case the residuals are large with small standard deviations. Based on these residuals or on residuals of verticality constraints the RPF can be relatively corrected to describe a consistent stereo situation with respect to derived DSM and orthoimages.

The standard deviations of the differences of RPF DSM heights and available (much coarser) DSM from InSar are in the order of the accuracies of the latter DSM.

Acknowledgement:

The authors acknowledge the manual measurements of tie points by Stephanie Beinhauer and Monika Harbich. Thanks go also to TU Munich for the laser DSM chip and the possibility to do the ground control measurements on the analytical plotter.

References:

Eisenbeiss, H., Baltsavias, E., Pateraki, M., Zhang, L., 2004. Potential of Ikonos and Quickbird imagery for accurate 3D point positioning, orthoimage and DSM generation. *International Archives of Photogrammetry, Vol 35, Part B*, 20th ISPRS Congress, Istanbul.

Grodecki, J., Dial, G., Lutes, J., 2004. Mathematical Model for 3D feature extraction from multiple satellite images described by RPCs. ASPRS Annual Conference Proceedings, Denver, Colorado

Heipke, C., Kornus, W., Pfannenstern, A., 1996. The evaluation of MEOSS airborne 3-line scanner imagery – processing chain and results, *Photogrammetric Engineering and Remote Sensing*, Vol. 62, No. 3, pp. 293-299

Müller, Ru., Lehner, M., Müller Ra., Reinartz, P., Schroeder, M., Vollmer, B., 2002. A program for direct georeferencing of airborne and spaceborne line scanner images, ISPRS, Commission I Mid-Term Symposium, Denver, CO, USA, 10-15 November 2002

Yamakawa, T., Fraser, C.S., 2004. The affine projection model for sensor orientation: experiences with high-resolution satellite imagery, *International Archives of Photogrammetry, Vol 35, Part B*, 20th ISPRS Congress, Istanbul.